Isomerization Dynamics and the Transition to Chaos

Bruce J. Berne,* Nelson De Leon, and R. O. Rosenberg

Department of Chemistry, Columbia University, New York, New York 10027 *(Received: July 20, 1981)*

Reaction dynamics in a Hamiltonian system with two degrees of freedom is studied as a function of the coupling strength between the reactive and nonreactive degrees of freedom. Rate constants and unimolecular phenomenology are shown to exist under certain conditions, but RRKM theory is valid only in systems that are "strongly stochastic". A statistical theory of reaction rates in nonergodic systems is constructed and the results are discussed in the context of this theory.

I. Introduction

Geometrical isomerization can be described by the motion of a reaction coordinate (often an internal angle) in a double or multiple potential well. For isomerization to occur, an isolated molecule must suffer an activating collision with a photon or another particle.[1] In a very dilute gas or in a molecular beam, the time between successive collisions may be made very long on the time scale of molecular vibrations. The subsequent dynamics of the activated molecule under collisionless conditions is of considerable interest. If the reaction coordinate is not coupled to other intramolecular degrees of freedom, the motion over the barrier will be periodic, rate constants will not exist, and the usual linear rate laws will be invalid. When the reaction coordinate is coupled to other intramolecular degrees of freedom, energy exchange between modes may or may not give rise to a linear rate law. If the coupling is sufficiently weak, the dynamics will still be quasiperiodic and will be described by motion on many-dimensional invariant tori in phase space.[2] In the KAM regime the usual rate laws will be invalid. It is shown here[3] that for weakly coupled two-dimensional systems, for energies above the barrier, the tori can be subdivided into two distinct classes: trapping tori (TT) and crossing tori (CT). Motion on CT corresponds to periodic crossing of the barrier with no trapping. As the "coupling"[4] is made stronger, there is a transition to "chaos" in which a measurable subset of CT are destroyed, but in which the TT are preserved. In this regime, motion over the barrier cannot get trapped in any of the wells. An important consequence of this is that again rate constants will not exist and the linear rate law will be invalid. As the coupling is further increased, more and more of the CT are destroyed until all of them are finally destroyed; only then do TT start getting destroyed. At this point, some of the trajectories which pass over the barrier get trapped for periods of time in one or another of the wells. This is a necessary condition for the existence of rate constants, and for the validity of linear rate laws. We are still uncertain as to whether it is a sufficient condition because, even though the motion is irregular, it displays a great deal of coherence whenever the trajectory visits regions of phase space near undestroyed TT. In these regions the irregular trajectories seem to trace out "vague tori" or "fuzzy tori" on the Poincaré surface of section. The correlations induced by the undestroyed TT have a very important effect on the reaction dynamics. In a qualitative sense, they act as "attractors", and induce the system to spend "long times" in their neighborhoods with the concomitant effect that these trajectories do not spend equal times in regions of the irregular part of phase space of equal microcanonical measure. For very strong coupling, almost all the CT and TT are finally destroyed. The trajectories are then highly stochastic and appear to visit regions of equal measure for equal times. In this regime it is clear that rate constants exist and, moreover, can be determined.

It follows from the foregoing that when the reaction coordinate is coupled strongly enough to other intramolecular degrees of freedom such that all of the TT and all CT are destroyed, energy exchange between the modes can give rise to linear rate laws and well-defined rate constants. If there is a very rapid equipartitioning of the energy between these modes, it might be expected that the RRKM theory applies and that the rate constant can be computed by using purely statistical arguments. In the moderate coupling regime, where all the CT are destroyed but where a measurable set of TT are preserved, the "non ergodicity" of the trajectories in the irregular region of phase space has the important consequence that a statistical theory of the rate constant will not suffice and a full dynamical theory will be required.

In this paper, we present a summary of a study of how the topological structure of phase space affects the chemical rate processes. First, we discuss RRKM theory and how it can be generalized to systems that are not ergodic. This discussion leads us to the question of how to determine rate constants in isomerizing systems. For this purpose we exploit the properties of the reactive flux. This is followed by a detailed study of a model system consisting of a bistable oscillator coupled to a Morse oscillator. It is shown that the lessons learned from this system are applicable to a more realistic system such as *n*-butane.

II. Statistical and Nonstatistical Theories of the Rate Constant

Consider motion on the two-dimensional potential energy surface given in Figure 1. The reaction coordinate, y, is coupled to an oscillator coordinate x, and energy can

* Invited Lecture at American Conference on Theoretical Chemistry, Boulder, CO, June, 1981.

(1) W. Forst, "Theory of Unimolecular Reactions", Academic Press, New York, 1973.

(2) (a) The role of the KAM theorem and the effects of chaos in dynamical systems has been discussed in connection with energy-transfer and dissociation in coupled oscillator systems. See the excellent reviews by D. W. Noid, M. L. Koszykowski, and R. A. Marcus, "Quasi-Periodic and Stochastic Behavior in Molecules, Physical Chemistry", Vol. 32, 1981; P. Brummer, *Adv. Chem. Phys.*, in press; I. C. Percival, *ibid.*, **36**, 1–61 (1977); S. A. Rice, *ibid.*, in press. For an excellent introduction to the various concepts in nonlinear mechanics, see J. Ford, *ibid.*, **24**, 155 (1972). (b) S. Nordholm and S. A. Rice, *J. Chem. Phys.*, **62**, 157 (1974).

(3) A large part of this lecture enlarges on N. De Leon and B. J. Berne, *J. Chem. Phys.*, **75**, 3495 (1981).

(4) Used here, the term coupling is a rather complicated quantity. It depends on the two parameters z and λ. Space does not allow us to make a clear statement of this quantity. Suffice it to say that the term coupling as used here is proportional to the measure of the irregular region of phase space.

0022-3654/82/2086-2166$01.25/0

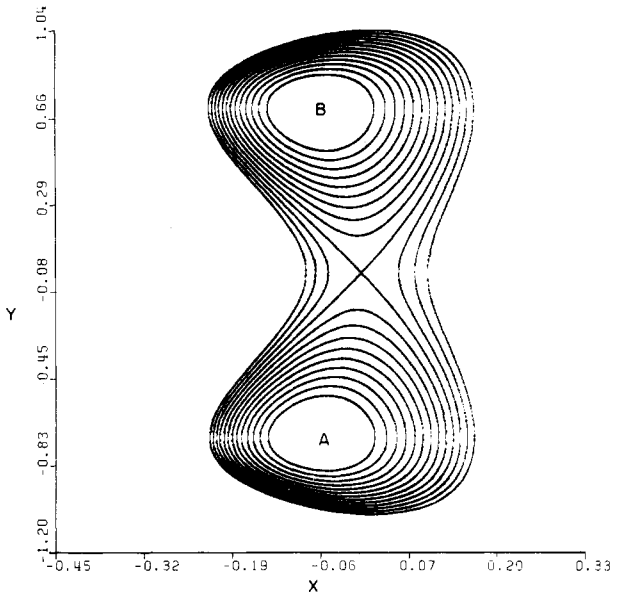

Figure 1. A representative potential energy surface for the Hamiltonian (cf. eq 3.1). The parameters for this particular surface are $z = 2.30$ and $\lambda = 1.95$. The transition state is located at $y = 0$. The reactants and products are labeled A and B.

be exchanged between these two degrees of freedom. The configuration space can be divided by the line ($y = 0$) into a reactant region denoted A and a product region B, and reactive trajectories must cross over the barrier. The saddle point ($x = 0$, $y = 0$) has an energy ϵ_0, and Figure 1 is the energy surface corresponding to a total energy $E \gtrsim \epsilon_0$, very close to this saddle point. It is important to recognize from the outset that the x width of the saddle point (the width of the "bottleneck") increases rapidly as E is increased. Since reaction rate constants will exist only if the "bottleneck" is sufficiently narrow to ensure long trapping times, compared to other "correlation times" in the system, let us first consider the case where E is very close to ϵ_0 ($E \gtrsim \epsilon_0$). We return to the higher energy states later.

The reaction can be described phenomenologically by

$$A \underset{k_b(E)}{\overset{k_f(E)}{\rightleftharpoons}} B$$

where $k_f(E)$ and $k_b(E)$ are the forward and backward rate constants at total energy E. Relaxation kinetics determine the kinetic rate constant

$$1/\tau_{rxn} \equiv k_f(E) + k_b(E)$$

This is the rate constant in the exponential time decay of an initial deviation from equilibrium. According to the fluctuation dissipation theorem of linear response theory,[5] a small deviation from equilibrium of the population in state B decays to equilibrium in precisely the same way as does the autocorrelation function of the spontaneous thermal fluctuations of the population; that is

$$\frac{\bar{N}_B(t) - N_B^0}{\bar{N}_B(0) - N_B^0} = \frac{\langle \delta N_B(0) \delta N_B(t) \rangle}{\langle \delta N_B(0)^2 \rangle} = C_B(t) \qquad (2.1)$$

If the phenomenological linear rate law is valid for all time, the left-hand side of this equation decays as e^{-t/τ_R} even at short times, and the autocorrelation function is a pure exponential. In this case, the kinetic rate constant $1/\tau_R$ can then be obtained

$$1/\tau_R = \lim_{t \to 0^+} (-dC_B(t)/dt) \qquad (2.2)$$

When the microscopic definition of $\delta N_B(t)$ is introduced derivatives taken, and time reversal invariance explored, it is possible to show that[6]

$$\frac{1}{\tau_R} = \frac{1}{x_A x_B} \langle \dot{y}(0) \delta(y(0) - y_c) \theta(\dot{y}(0)) \rangle \qquad (2.3)$$

where x_A and x_B are the equilibrium mole fractions of A and B, $y = 0$ is the value of the reactive coordinate (ordinate in Figure 1) corresponding to the barrier maximum, $\dot{y}(0)\delta(y(0) - y_c)$ is the flux over the barrier, ($y_c = 0$), and $\theta(\dot{y})$ is the unit step function specifying that $\dot{y} > 0$. The step function counts only trajectories moving from A to B. The $\langle ... \rangle$ indicates an average over either a microcanonical or a canonical ensemble. According to eq 2.3 all trajectories initially passing over the barrier and moving from A to B contribute to the rate constant—even trajectories that might during the next instant recross the barrier. This formulation of the rate constant will be rigorously valid only if every trajectory crossing the barrier gets trapped for a long time in a well before it can recross the barrier. This can happen only if there is a very rapid energy equipartitioning between the reactive degree of freedom and the other modes. Thus the assumption of a single exponential decay implies a dynamic model in which there is no rapid recrossing of the barrier; i.e., it implies rapid energy equipartitioning.

If the ensemble used is a constant temperature ensemble (a canonical ensemble), the predicted kinetic rate constant, $1/\tau_R$, as given by eq 2.3, is the transition-state rate constant, i.e., $1/\tau_R \equiv 1/\tau_{TST}$. If the ensemble used here is the constant energy ensemble (the microcanonical ensemble), the rate constant obtained is the *RRKM* rate constant, i.e. $1/\tau_R \equiv 1/\tau_{RRKM}$

$$\frac{1}{\tau_{RRKM}} = \frac{\int d\Gamma\ \delta(E - H(\Gamma)) \dot{y} \delta(y - y_c) \theta(\dot{y})}{\int d\Gamma\ \delta(E - H(\Gamma))} \qquad (2.4)$$

where we have explicitly expressed $\langle \dot{y}\delta(y - y_c)\theta(\dot{y}) \rangle_E$ as an average over the microcanonical distribution function

$$\rho(\Gamma) = \frac{\delta(E - H(\Gamma))}{\int d\Gamma\ \delta(E - H(\Gamma))} \qquad (2.5)$$

Here Γ denotes a point in phase space; that is, a microscopic state of the system (all positions and conjugate momenta), $H(\Gamma)$ is the Hamiltonian evaluated at Γ, and

$$\Omega(E) = \int d\Gamma\ \delta(E - H(\Gamma)) \qquad (2.6)$$

is the density of classical states. Clearly the RRKM theory implies that all classical states in the energy shell are accessible to the system, and moreover all of these states are equally probable.

The RRKM rate constant depends on an equilibrium microcanonical average. It is a purely statistical theory, and as such the RRKM rate constant contains no dynamical information. The dynamics are hidden in the initial assumption that the correlation function decays as a single exponential over all time, or, concomitantly, that a trajectory crosses the barrier and gets trapped for long periods of time before recrossing. Implicit in this is the assumption that there is no correlation in the times spent trapped in each well. Of course, these dynamical assumptions are very

(5) See, for example, D. Forster, "Hydrodynamic Fluctuations, Broken Symmetry and Correlation Functions", W. A. Benjamin, New York, 1975.

(6) D. Chandler, *J. Chem. Phys.*, 68, 2959 (1978).

restrictive and we will return to them later.

Because RRKM theory plays a very important role in the theory of chemical kinetics and in the interpretation of experiments, it is worth considering the circumstances under which it breaks down. If conditions are such that the energy hypersurface, $H(\Gamma) = E$, is metrically decomposable into regular and irregular regions, then any given trajectory crossing the barrier will not be able to visit some measurable regions of phase space. The motion will then be nonergodic and any statistical theory, such as RRKM theory, which assumes ergodicity will be in error. As pointed out in the Introduction, the mechanical system studied in this paper has the property that, for moderate coupling strength between the reactive and nonreactive degree of freedom, the phase space decomposes into a regular region consisting only of trapped tori (TT) and an irregular region in which all the crossing tori (CT) and some of the TT are destroyed. Thus all of the reactive trajectories, that is, all of the trajectories that can cross the barrier are irregular. Because some TT are destroyed, some of these reactive trajectories can get trapped. If one assumed that all states in the irregular region of phase space are equally probable, it is a simple matter to derive a modified statistical theory of the rate constant.[3] The details are given in Appendix A. This leads to a rate constant $1/\tau_{BD}$ for a symmetric double well:

$$\frac{1}{\tau_{BD}} = \frac{\Omega(E)}{\Omega_{irr}(E)}\left(\frac{1}{\tau_{RRKM}}\right) \tag{2.7}$$

where we assume that all crossing tori have been destroyed by the coupling, and where

$$\Omega(E) = \int_{\text{all }\Gamma} d\Gamma\ \delta(E - H(\Gamma)) \tag{2.8a}$$

$$\Omega_{irr}(E) = \int_{\text{irreg }\Gamma} d\Gamma\ \delta(E - H(\Gamma)) \tag{2.8b}$$

are respectively the full density of states at energy E and the density of states counting only the irregular region of the energy hypersurface. Obviously

$$\Omega_{irr}(E) \leq \Omega(E) \tag{2.9}$$

$$1/\tau_{BD} \geq 1/\tau_{RRKM} \tag{2.10}$$

In this modified RRKM theory it is assumed that a trajectory starting at the barrier can visit all parts of the irregular region of phase space; that is, the motion in the irregular region must be "ergodic" in the sense that the trajectory spends equal times in irregular regions of equal measure.

In the system studied in subsequent sections (particularly section 3), it is found that as the coupling strength between the reactive degree of freedom and the nonreactive degree of freedom is made larger, the measure of the irregular region grows, and concomitantly $\Omega_{irr}(E)$ approaches $\Omega(E)$. Thus we expect that $1/\tau_{BD}$ (expressed in units of $1/\tau_{RRKM}$) should decrease with coupling strength as shown schematically in Figure 2. This is a definite prediction of our statistical theory. It will be shown that this behavior is contrary to observation.

Even in a system where all the trajectories are irregular, RRKM theory becomes a poor approximation if there is correlated motion across the barrier or if there are short-time recrossings of the barrier. (Even in fully stochastic models of barrier crossings, there can be substantial deviations from RRKM theory.) Then the correlation function will not be a single exponential, and the rate constant will depend on dynamics and will not be given by a statistical theory or our modification of it.

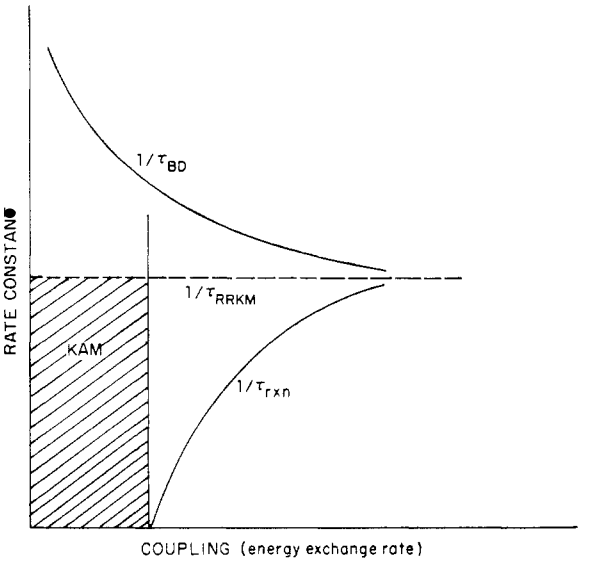

Figure 2. A schematic diagram of the dependence of the reaction rate $1/\tau_{rxn}$ on the coupling strength (or energy exchange rate). The curve labeled $1/\tau_{rxn}$ refers to the long time exponential decay rate determined from the reactive flux. $1/\tau_{RRKM}$ refers to the rate predicted from RRKM theory. It is not sensitive to coupling strength (see Table I). The term "coupling strength" should not be confused with perturbation strength.[3] $1/\tau_{BD}$ is the rate predicted by the statistical theory (RRKM-like theory) applied only to the irregular part of the energy hypersurface. See eq A7b.

A simple model provides much insight into how dynamical effects might influence the rate constant. Let us define the rate constant for energy exchange between the reactive degree of freedom and the nonreactive degrees of freedom as γ (should an energy exchange rate exist). We expect that γ will be an increasing function of the coupling strength between modes. Now consider a trajectory that crosses the barrier. If γ is small, this trajectory will recross the barrier many times before losing energy to the "nonreactive" degrees of freedom (i.e., to the bath). It will then librate in a well until it can regain enough energy to recross the barrier. Thus it remains trapped for a time γ^{-1}. Since the rate constant is inversely proportional to the trapping time, $1/\tau_{Rxn}$ is directly proportional to γ. Thus $1/\tau_{Rxn}$ should be an increasing function of the coupling as shown schematically in Figure 2. Clearly there is a strong disagreement between a statistical approach and a dynamical approach.[7] It is important to emphasize that dynamical effects give rise to rapid recrossings of the barrier and to nonexponential decay of the correlation function.

It is worth pointing out here that the absence of rapid recrossings of the barrier is a necessary but not sufficient condition for the validity of a statistical theory. If the times spent trapped in either well are correlated, there will be a nonexponential decay, and the initial rate of decay of $C_B(t)$ will not determine the long time rate of decay. It is the long time decay of $C_B(t)$ that gives the rate constant. An extreme illustration of this is given by a model in which the trapping times are long but are identical for each well. Then the reactive trajectories will be completely periodic. If there is some distribution of periods, $C_B(t)$ will exhibit an oscillatory decay. In these cases, the relaxation is highly inhomogeneous, and the usual chemical kinetic phenomenology will not apply. A necessary and sufficient condition for the existence of rate constants is that at long

(7) This model is similar in spirit to the stochastic model studied in J. A. Montgomery, Jr., D. Chandler, and B. J. Berne, *J. Chem. Phys.*, **70**, 4056 (1979).

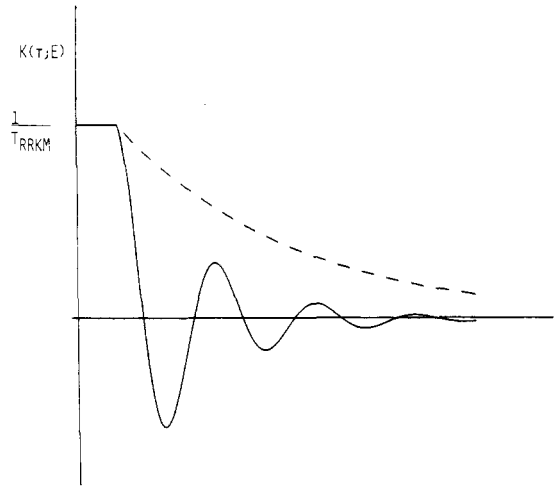

Figure 3. A schematic diagram indicating how the reactive flux evolves in time under two extreme conditions. The dashed curve corresponds to the case when the energy correlation time, γ^{-1}, is much shorter than $\tau(E)$, the period for crossing the well. The solid curve corresponds to the case where γ^{-1} is long compared to $\tau(E)$.

times $C_B(t)$ should decay exponentially.

To proceed with a thorough study of reaction dynamics, it is essential that we devise a method for determining whether reaction rate constants exist, and for evaluating these rate constants. How then can these rate processes be studied efficiently? Fortunately, there already exists a method of analysis based on the fluctuation dissipation theorem.[6-8] To this end we define the quantity

$$k(t) \equiv -\mathrm{d}C_B(t)/\mathrm{d}t = \langle \dot{y}(0)\delta(y(0))\theta(y(t))\rangle \quad (2.11)$$

The quantity on the right contains the step function θ which is unity if at time t, $y(t)$ is to the right of the barrier; that is, if the system is on the product side of the well, i.e., in the B state. As before, $\dot{y}(0)\delta(y(0))$ is the incident flux over the barrier ($y(0) = 0$). Thus $\dot{y}(0)\delta(y(0))\theta(y(t))$ represents that part of the initial flux over the barrier which at time t is in state B. The bracket indicates an ensemble average over either a constant T or constant E ensemble. In the latter case $k(t)$ is denoted $k(t;E)$. This is the "reactive flux".

Two important features of $k(t;E)$ are[6-8] (a) $\lim_{t\to 0^+} k(t;E) = 1/\tau_{RRKM}$ and (b) should rate constants exist, $\lim_{t\to\infty} k(t;E) = \to e^{-t/\tau_{Rxn}}$. Thus from the short time behavior, we can determine $1/\tau_{RRKM}$ and from the long time behavior of $k(t;E)$, we can determine the rate constant $1/\tau_{Rxn}$—should it exist.

The dynamical behavior of the microcanonical reactive flux is schematically illustrated in Figure 3 for a two well problem. The initial value of $k(t;E)$ is $1/\tau_{RRKM}$. In a microcanonical ensemble, the shortest time required for a trajectory to cross one well and return to cross the barrier is denoted $\tau(E)$. Thus the reactive flux is constant for this period of time. The dashed curve corresponds to the case where the energy exchange rate, γ, is sufficiently large that most of the trajectories do not have sufficient time to recross the barrier before losing energy to the other modes. In this case $k(t;E)$ looks exponential. The solid curve represents the opposite case where γ is sufficiently small that the trajectories can recross many times before losing energy. This gives rise to a dephasing oscillatory decay reminiscent of inhomogeneous relaxation. In this case, rate constants do not exist.

(8) R. O. Rosenberg, B. J. Berne, and D. Chandler, *Chem. Phys. Lett.*, 75, 162 (1980).

To compute the reactive flux, one simply (microcanonically) samples initial phase points such that, in all of them, the system is at $y(0) = 0$. The trajectories corresponding to these initial states can then be used to determine the reactive flux. (See ref 3 for details.) In addition, since each of these trajectories originates at $y = 0$, it is possible to determine the first time at which they recross $y = 0$. The distribution of first passage times, $p(\tau)$, can then be determined, and from this distribution the fraction, $W(\tau)$, of trajectories which have not made a first passage between 0 and τ can be determined. These distributions give further insight into the reaction dynamics. For example, from the unimolecular rate law, it is possible to show that a molecule will remain trapped in a well for time τ with probability, $e^{-k\tau}$, where k^{-1} is the mean lifetime in the well. The rate law therefore implies that the trapping times are "randomly" distributed. Any deviation from a random distribution indicates a breakdown of RRKM theory and possibly unimolecular phenomenology.

3. The Dynamical Structure of Phase Space for an Isomerizing System

It is the aim of this paper to clarify the conditions under which isomerization dynamics in isolated molecules gives rise to unimolecular rate laws and rate constants. Moreover, it is of interest to ascertain when, if ever, statistical theories such as the RRKM theory apply.

To clarify the above questions, we study the dynamical behavior of a classical system with the Hamiltonian

$$H = 4(\dot{x}^2 + \dot{y}^2) + 4y^2(y^2 - 1)e^{-z\lambda x} + \tilde{D}_0(1 - e^{-\lambda x})^2 + 1 \quad (3.1)$$

The potential[9] represents a quartic bistable potential (in y) with energy barrier $e^{-z\lambda x}$ coupled to a Morse oscillator (in x). The coupling arises from the dependence of the barrier height[4] on x, the displacement from equilibrium of the Morse oscillator. Energy is measured in units of the barrier height corresponding to $x = 0$. $\tilde{D}_0$ is the dissociation energy of the Morse oscillator in these units, and λ is the range parameter of the Morse potential. The quartic has two minima (stable points) at $y = \pm(1/2)^{1/2}$ and a maximum (metastable point) at $y = 0$. These extremal points, and therefore the saddle point ($x = 0$, $y = 0$), do not depend on x. In what follows, we fix $\tilde{D}_0 \equiv 10$. This is consistent with our expectation that, in any real molecule, the dissociation energy will be much larger than the barrier to internal rotation. Thus we will study the Hamiltonian flow as a function of the coupling parameter z and the Morse parameter λ.

The Hamiltonian of the system, eq 3.1, can be expressed as

$$H = H_0(x) + H_0(y) + V(x,y) \quad (3.2)$$

where

$$H_0(x) = 4\dot{x}^2 + \lambda_3(1 - \exp(-\lambda x))^2 \qquad \lambda_3 \equiv D_0/\epsilon_2 \quad (3.3a)$$

$$H_0(y) = 4\dot{y}^2 + 4y^2(y^2 - 1) + 1 \quad (3.3b)$$

$$V(x,y) = 4y^2(y^2 - 1)[\exp(-z\lambda x) - 1] \quad (3.3c)$$

The classical motion of the unperturbed nonlinear oscillators $H_0(x)$ and $H_0(y)$ can be solved analytically. It is important to note that only $H_0(y)$ is independent of the parameters λ,z. Thus as λ,z are varied, most of the

(9) This model springs from the expectation that the barrier to internal rotation in a real molecule will decrease when the bond connecting the rotation groups is stretched. For example, in ethane the barrier to rotation of CH_3 should decrease as the C–C bond is stretched. In butane, the barrier in the gauche $\rightleftarrows$ trans isomerization should decrease as the C2–C3 bond is stretched or if the C–C–C angles are stretched.

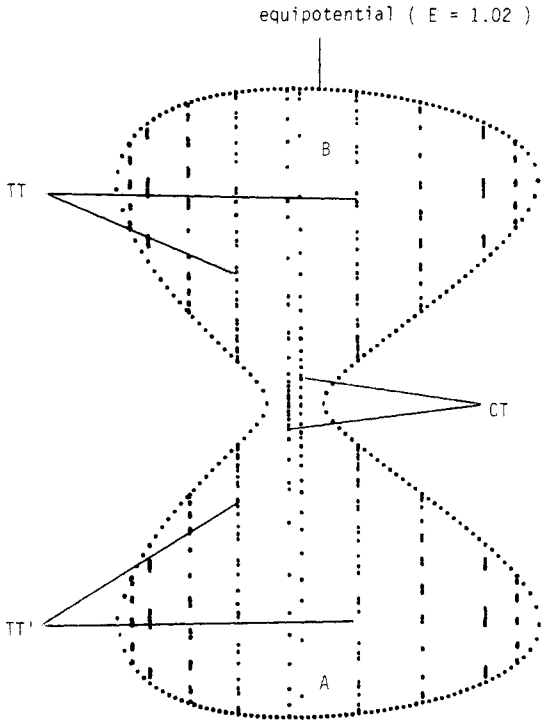

Figure 4. Configurational surface of section (CSS): This example of a configuration surface is ($z = 0$) at an energy $E = 1.02\epsilon_0$ and $\lambda = 1.0$. TT and TT′ correspond to trapped tori and CT corresponds to a crossing torus.

structural deformation of the potential surface will occur along the nonreactive degree of freedom x.

It is interesting to note that the ratio of the frequency of the uncoupled Morse oscillator to that of the uncoupled bistable oscillator is

$$R_\omega = \lambda_3^{1/2}\left\{\frac{1 - [(E-1)/\lambda_3]^{1/2}}{2\omega_B{}^0}\right\}\lambda \qquad (3.4)$$

Taking $\lambda_3 = 10$, $E = 1.02$, and $\omega_B{}^0$ just below the barrier give

$$R_\omega = 3.5\lambda \qquad (3.5)$$

This gives a "ballpark" estimate of the number of oscillations of the Morse oscillator, corresponding to one oscillation of the reactive degree of freedom. As we shall see, the qualitative behavior of our system can be correlated with R_ω.

In discussing Hamiltonian flows in nonlinear dynamics it has proved useful to map the trajectories onto particular two-dimensional surfaces. These Poincaré surfaces of section, PSS, reveal the underlying dynamical structure of the system. In a previous paper[3] we define a surface of section not previously introduced in the literature. It is simply a mapping of the trajectories onto a configuration plane rather than onto the usual coordinate-conjugate momentum plane. It is constructed as follows: When the morse oscillator is at a turning point $\dot{x} = 0$, the position of the system (x,y) is recorded by a point in configuration space. The advantage of this "configurational surface of section" (CSS) is that it readily gives a physical picture of what parts of configuration space a trajectory may visit.

Consider the CSS of Figure 4 corresponding to the totally uncoupled system ($z = 0$). The outer contour in this figure corresponds to the equipotential $V = E = 1.02\epsilon_0$. The energies in the x and y degrees are separately conserved. Each trajectory has a mapping which is a pair of approximately parallel lines (dots if the trajectory is followed for finite times). The x component of these two lines gives the turning points of the Morse oscillator. Such a pair of lines corresponds to a two-dimensional invariant torus in phase space (defined by two isolating integrals of motion). Motion on these tori is periodic or quasiperiodic. We note that these tori can be subdivided into two classes:

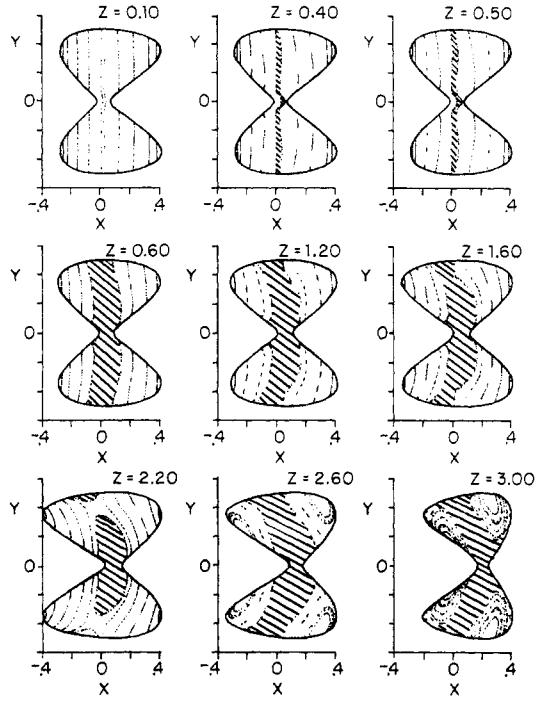

Figure 5. A series of configurational surfaces of section are displayed. The various systems are at a total energy of $1.02\epsilon_0$, with the same Morse parameter λ (= 1.0), and varying perturbation strength z. Hatched regions correspond to regions of configuratrion space accessible to unstable reactive trajectories. The region outside the hatched zone is filled with trapped tori, and is thereby inacessible to crossing trajectories. One tic mark along the y axis corresponds to 0.4 dimensionless units.

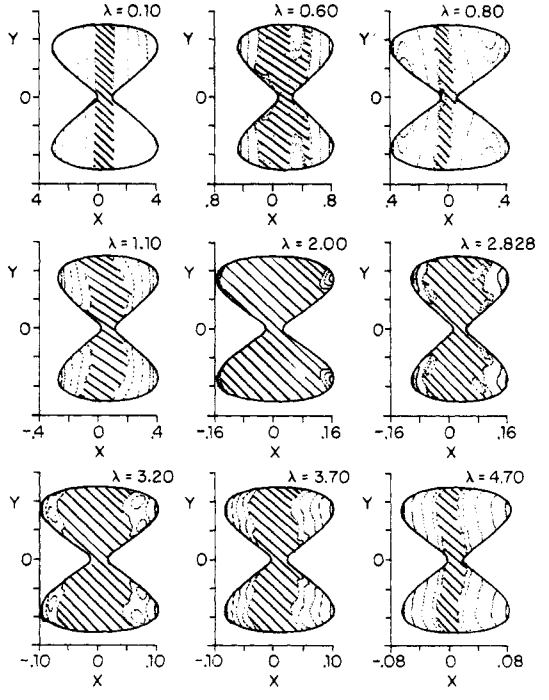

Figure 6. A series of configurational surfaces of section are displayed. The various systems are at a total energy of $1.02\epsilon_0$, with the same value of the perturbation strength z (= 1.0), but varying λ. The hatched regions are explained in Figure 5. One tic mark along the y axis corresponds to 0.4 dimensionless units.

crossing tori (CT) and *trapped tori* (TT). On the former, $y(t)$ periodically moves back and forth across the barrier, whereas on the latter $y(t)$ is trapped forever in either well. The trapped tori each consist of a pair of parallel lines that are separated by a distance, Δx, greater than the x width of the saddle point region, as indicated on Figure 4.

What happens to the structure of these invariant manifolds is shown in Figures 5 and 6. In Figure 5 the energy is fixed at $E = 1.02\epsilon_0$ (slightly above the barrier), λ is fixed at $\lambda = 1.0$, and z is varied from 0 to 3.0. For z sufficiently small ($z \sim 0.10$), the system is in the KAM region—"all" tori are preserved but those crossing the "transition state" are distorted. As z increases, first a narrow band (indicated by the thatched region) of CT is destroyed and trajectories in this region are irregular. A measurable set of CT and all TT are still preserved. For $z > 0.60$, all the CT are destroyed and some TT are preserved.

In Figure 6, the energy is again fixed at $E = 1.02\epsilon_0$, z is fixed at $z = 1.0$, and λ is varied from 0.10 to 4.70. The coupling $z = 1$ is strong enough that in all of these sections there is a stochastic region (indicated by a cross-matched region). A quick view of Figure 6 shows that as λ is varied from 0.1 to 4.7 the region of stochasticity grows, shrinks, grows, and then shrinks again. From eq 3.5 it is seen that, when λ is very small, y varies very rapidly compared to x; thus y can adiabatically follow x. When λ, and correspondingly R_ω, is very large, the converse is true, and x can adiabatically follow y. In both these extremes an adiabatic invariant will exist and the enrgy hypersurface should be filled with tori. This is precisely what is found, although it is not indicated in the figure. As one moves from the adiabatic region corresponding to low R_ω, the tori near the barrier are first deformed and a thin ribbon of stochasticity sets in. This region grows as R_ω is increased further, becoming a substantial fraction of the section around $\lambda = 2.00$. We expect that, as R_ω is further increased, the region of stochasticity will decrease until finally for very high R_ω, when adiabadicity sets in, the plane is filled with tori. Actually, there is a region around $0.6 < \lambda < 1.0$ when the stochasticity diminishes and then increases. This behavior is rather unexpected and merits further study. It shows that the degree of stochasticity is a sensitive function of the parameters of the system.

These observations can be summarized as follows:

(1) The phase space of an isolated weakly coupled system exhibiting isomerization is decomposable into crossing tori (CT) and trapping tori (TT).

(2) CT are less stable than TT. Thus for intermediate coupling only a subset of the CT are destroyed. The TT are preserved, and the motion over the barrier, although irregular, never exhibits trapping.

(3) For strongly coupled systems, a measurable set of TT get destroyed, and crossing trajectories can get trapped. In this case, it is important to recognize that these irregular trajectories can visit only those regions of phase space not occupied by tori. This "excluded volume" effect may introduce strong correlations in the system.

(4) Increasing z at fixed λ has a limited effect on the system. In Figure 5 varying z over its full range for $\lambda = 1$ does not destroy all the TT.

(5) Frequency variations (λ variations) have a much more pronounced effect on the dynamical structure than do increases in the perturbation strength z.

(6) If in the uncoupled system one mode is much faster than the other mode, then in the coupled system the two modes will be adiabatically decoupled.

(7) We can expect to see linear rate laws in systems in which there is a high degree of stochasticity; that is, in systems where the natural periods in the decoupled system do not differ too much.

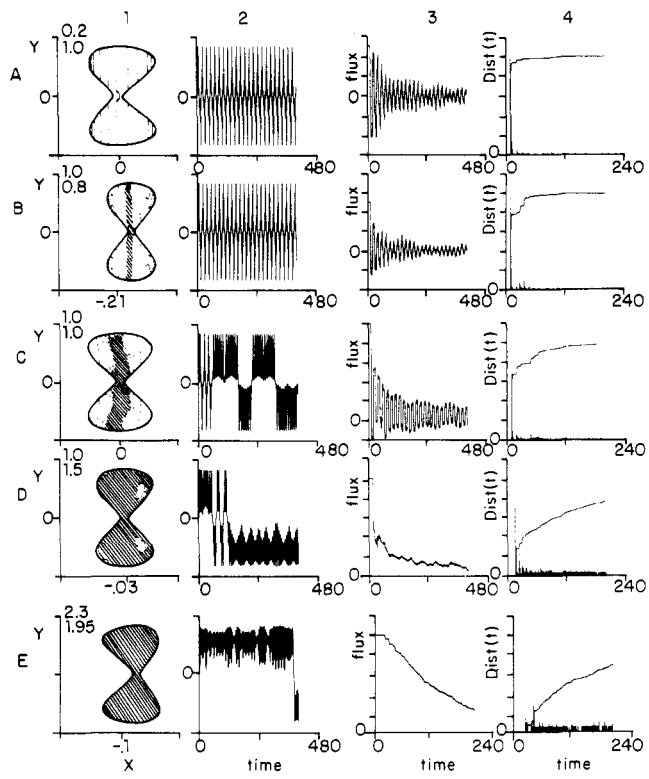

Figure 7. Overview of representative systems: A comparison of the configurational surface of section, the time evolution of the reactive coordinate $Y(t)$, the flux, and the distribution of first passage times $W(T)$ is given. Along the ordinate, one tic mark corresponds to 1.2 units in columns 1 and 2, 0.4 units in A3 and B3, 0.2 units in C3, D3, and E3. In column 4, the units along the ordinate are arbitrary. The upper left hand corner of column 1 gives the values of z (top) and λ for each system.

It is important to note that because the measure of the irregular region of phase space is a very sensitive function of the parameters, the statistical rate constant (cf. eq 2.7) will be a very sensitive function of the parameters λ,z.

4. Reaction Dynamics in a Two-Dimensional System

The simple Hamiltonian system has a very rich dynamical structure. It is of considerable interest to relate the isomerization dynamics in this system to the structure in phase space as indicated in the CSS. The reaction dynamics in a representative set of systems is summarized in Figure 7. Column 1 gives a set of CSS at $E = 1.02\epsilon_0$, corresponding to different parameter choices (λ,z). The hatched areas indicate stochastic regions. Column 2 gives a set of representative crossing trajectories. Column 3 gives a set of microcanonical reactive fluxes and column 4 gives a set of first passage time distributions. Each row corresponds to a given system (λ,z) in the CSS. As one goes from row A to row E, the systems get more stochastic; that is, the nonlinear coupling gets stronger. System A is weakly coupled; all the trajectories are regular, and the phase space (or CSS in A1) is entirely decomposable into crossing tori (CT) and trapping tori (TT). The representative trajectories are quasiperiodic, and a typical crossing trajectory (Figure 7A2) has the reactive coordinate periodically crossing the barrier. In system B, the coupling is strong enough to destroy "all" of the crossing tori; thus the crossing trajectories must be irregular; nevertheless, the reaction coordinate looks rather periodic (Figure 7B2). In neither system A nor B do we observe trapping. In system C the coupling is strong enough to destroy some

TT. This should be obvious from the fact that the stochastic strip is now wider than the transition zone. Now the representative trajectory moves across the barrier and gets trapped for many librational periods before recrossing the barrier. The librational motion looks coherent. In system D, a very large measure of the TT are destroyed, the representative trajectory gets trapped for long periods of time, but there still seems to be a great deal of coherence in the trapped motion. Finally in system E, all the tori are destroyed. Now the crossing trajectory gets trapped for a very long period of time and, moreover, the librational motion looks very chaotic.

It is clear from column 2 of Figure 7 that in systems C and D the crossing trajectories are irregular; but, nevertheless, portions of the trapped motion look quite coherent. These trajectories show a very high degree of correlation. For example, when the system crosses the barrier, it seems to recross it several times, but when it gets trapped, it seems to librate quite coherently. Could this arise because these trajectories evolve on some remnants—so to speak—of a crossing torus and then switch over to a remnant of a trapping torus? It is almost as if the irregular trajectory is captured for a time by the surviving tori and moves under their influence; that is, moves, so to speak, on a "vague torus".[10] Should this be the case, then as more and more trapped tori are destroyed, the coherence and concomitant long correlation times should disappear. In Figure 7E2, we see that the reactive trajectory looks very random—very much like it would if it was strongly coupled to a heat bath. Here no tori survive so the irregular crossing tori never fall under the influence of tori and the motion is very chaotic.

To test these ideas, we show in Figure 8 the usual Poincaré surface of section (PSS). Here the trajectories are mapped onto the $(y,\dot{y})$ plane whenever $x = 0$, $\dot{x} > 0$. Closed curves in this plane indicate tori. In Figure 8A1 we show the mapping of the irregular crossing trajectory (cf. Figure 7B) onto the PSS. The irregular behavior occurs mainly near the saddle point. The motion is nevertheless quite coherent, and the mapping looks, in fact, very similar to a pure crossing torus in the uncoupled system. In Figure 8A2 the solid curve indicates the outer trapped torus. The dots are the mapping onto the PSS of the irregular crossing (reacting) trajectory given in Figure 7C. It should be noted that, during this period of time, the irregular trajectory follows the trapping torus very closely. The motion is quite coherent. In Figure 8B1 the regions (indicated by (A), (B)) define two topologically distinct tori. The dots about region A and B are formed by the two independent trajectories 8B11 and 8B22, respectively. Only the very regular part of trajectory 8B11 (the part between the arrows) was used to obtain the dots on the PSS. The fact that these two irregular trajectories seem to move for very long periods of time, in a very localized region of phase space, is surprising. This short time structure so closely resembles motion on a surviving torus that this can be called a "vague torus". In fact, the trajectory labeled 8B22 moves on a "vague torus"[10] resembling torus A. Though not shown here, other trajectories seem to "jump" periodically from the A torus to the B torus. Trajectories influenced by tori in A or B execute many periods before wandering away and visiting the hatched regions in Figure 8B. In the hatched region, the motion becomes more chaotic. The amplitude, $y(t)$, then becomes more irregular. Could it be that the hatched areas contain regions of negative Riemanian curvature?[11] This decomposition is approximate in that eventually a trajectory starting in one such region does indeed visit the other region. Nevertheless, the long correlation times associated with certain kinds of motion arise from this "nonhomogeneity" of the irregular part of the energy hypersurface. Lastly, in Figure 8B2 the mapping of the very "stochastic" trajectory of Figure 7E is shown. This is the typical "shotgun" pattern usually associated with the stochastic instability.[12] Here no evidence of dynamical structure is observed. These observations appear to suggest the existence of "vague tori" and lead us to conjecture the following:

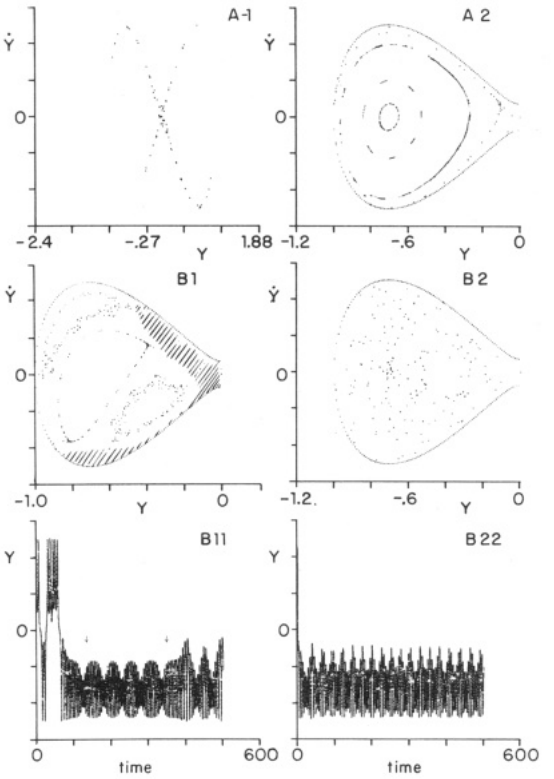

Figure 8. The surface of section in A2, B1, and B2 correspond to only the reactant "A" side of the potential energy surface. In B1, A and B correspond to distinct trapped tori (A is the inner torus (oval) and B corresponds to the outer two ovals). The trajectories B11 and B22 were used to obtain the "vague" tori A and B in B1, respectively. The arrows in B11 indicate where the trajectory was "cut" in order to obtain the section. Note the regularity of the amplitudinal motion in both cases—even though they are "supposed" to be irregular. One tic mark along the ordinate in parts B11 and B22 correspond to 0.4 units. All other tic marks along the ordinate are 0.2 dimensionless units.

Systems in which not all the invariant tori are destroyed have a measurable set of irregular trajectories that spend finite, and relatively long, periods of time executing almost regular motion. This quasi-regular motion occurs when the trajectories visit irregular regions of phase space neighboring existing tori. Approximate invariants may exist in these regions—hence they have been called vague tori. Trajectories in these regions are quite stable and lead to long correlation times and trapping times.

The reactive flux $k(t;E)$ (cf. eq 2.11) corresponding to Figure 7 were each computed by averaging over microcanonically sampled trajectories. These are presented in Figure 7A3–E3. The trajectories were computed by using the De integrator based on the Adams Moulton algorithm.[13] Integration accuracy was monitored by conser-

(10) W. Reinhardt, privation communication. (See Reinhardt's lecture.)

(11) Yoji Aizawa, *J. Phys. Soc. Jpn.*, **33**, 1963 (1972). R. Kosloff and S. A. Rice, *J. Chem. Phys.*, **74**, 1947 (1981).

(12) M. Henon and C. Heils, *Astron. J.*, **69**, 73 (1964).

vation of total energy with % error = 0.01, and by time reversal. The computations were carried out in double precision on a VAX 11/780 computer. The sampling techniques and other details of the calculation are discussed in ref 3.

Since each of the trajectories originates at $y = 0$, it is possible to determine the first time at which they recross $y = 0$, and thereby the distribution of first passage times, $p(\tau)$, and the corresponding fraction, $W(t) \equiv 1 - \int_0^t dt\, p(\tau)$, of trajectories which do not make their first passage before time t. These are given in Figure 7A4–E4.

The histograms, $p(\tau)$, show that there is a minimum time for first passage. This corresponds to the shortest time for traversal of a well at the fixed energy E. Moreover, they show that there are fairly well-defined narrow short time peaks. These represent the trajectories that do not get trapped but instead recross the transition state quickly, and with a very small dispersion in first crossing times. This is expected in systems with weak coupling, where the system is not stochastic, but it should be noted that there is a remnant of this rapid recrossing even in the systems in which all reactive trajectories are "stochastic". The fraction of trajectories that rapidly recross decreases as the coupling increases; nevertheless, even in very stochastic systems, there is a high degree of coherence typified by the narrow peak. In addition, we see that the distribution of "long first passage times" is quite broad. The probability of not making a first passage in time t is also given in Figure 7A4–E4. In the fully "stochastic" system, the long time behavior of this distribution looks quite exponential—a result consistent with a "random" or Poisson distribution of first passage times—a signature of a unimolecular rate law. In the less stochastic systems, the long time behavior is consistent with a sum of two or more exponentials, so that only at times much longer than given in Figure 7B4–D4 will it be possible to determine the rate constant. The reason for this long time behavior appears to be that the trajectories seem to get coherently trapped for very long times on "vague trapping tori", i.e., remnants of the trapping tori. Thus an accurate determination of the long time decay might give smaller values of $1/\tau_{Rxn}$ than are reported here.

The reactive flux given in Figure 7A3–E3 are completely consistent with the above discussion. When there is weak coupling, $k(t;E)$ exhibits a decay due to dephasing. Each reactive trajectory is essentially periodic in $y(t)$, but there is a distribution of periods (given by the sharp peaks of $p(\tau)$). As the coupling gets stronger, the first peak in $p(\tau)$ decreases and the fraction of trajectories giving rise to "random" recrossing time grows. Since the former gives "heterogeneous oscillatory decay", and the latter "exponential" decay, the flux behaves something like the superposition of these two kinds of decays. The behavior is of course more complicated than this description would imply. Thus in the case of strong coupling, the long time decay is "exponential" and a rate constant can be extracted.

The τ_{RRKM}^{-1} were computed analytically from eq 2.11. It is found that *there is agreement between* τ_{Rxn}^{-1} *and* τ_{RRKM}^{-1} *only from the most stochastic systems* (Figure 7E) where $\tau_{Rxn}^{-1} = (7.5 \pm 0.5) \times 10^{-3}$ and $\tau_{RRKM}^{-1} = 7 \times 10^{-3}$. Clearly, when the measure of trapped tori is nonzero, the reactive trajectories are restricted to a subregion of the energy hypersurface and the density of states used in RRKM overcounts the reactive states. Then RRKM will be a very poor approximation. As discussed in section I and Appendix A, the statistical theory can be modified by considering the irregular region of phase space; cf. eq 2.7 and eq A.7. The modified rate constant τ_{BD}^{-1} satisifes the inequality given by eq 2.10. Thus we expect that as the coupling (stochastic region) increases, $(\tau_{BD})^{-1}$ decreases until it eventually becomes equal to τ_{RRKM}^{-1}. This happens when the whole energy hypersurface is stochastic. It is $(\tau_{BD})^{-1}$ which gives an upper bound on the actual rate constant τ_{Rxn}^{-1}. We have found that τ_{Rxn}^{-1} increases with stochasticity. Thus neither the full nor the modified RRKM (TST) theory accounts for the "experimental" results when there is not full stochasticity. The situation is summarized schematically in Figure 2. Instead, the rate constant τ_{Rxn}^{-1} depends on dynamical properties (like the energy exchange rate). This bears a close resemblance to what happens in stochastic theories where the rate constant depends on dynamic properties, like the collision rate or friction coefficient, and only becomes equal to the transition-state value under rather restrictive conditions. Another possible explanation is that, in the less stochastic systems, motion on "vague tori" give rise to long trapping times.

The above observations can be summarized as follows:

(i) The measure (in the Lebesque sense) of the irregular part of the energy hypersurface must be close to the measure, $\mu(E)$, of the constant energy surface, that is, a significant fraction of the TT must be destroyed before one can expect to observe linear rate laws.

(ii) For very strongly coupled systems, that is, systems in which all the tori are destroyed, a unimolecular rate law pertains, rate constants exist, and these rate constants are moreover very well approximated by RRKM (transition state) theory.

(iii) In less strongly coupled systems, that is, systems in which trapping tori still exist, it appears that a unimolecular rate law describes the behavior of the reactive trajectories, but now the rate constants are not approximated by the full RRKM theory. A modified RRKM theory taking account of the restricted density of states corresponding to the stochastic region of phase space gives very poor agreement with the dynamics. In fact, we find that $1/\tau_{Rxn}$ increases with stochasticity, whereas $1/\tau_{BD}$ decreases with stochasticity.

(iv) At intermediate coupling, there appears to be a high degree of correlation in the irregular trajectories. This correlation seems to be related to the regions of phase space still occupied by tori. When an irregular trajectory comes near a region occupied by tori, it behaves coherently; when it is in regions free of tori, it behaves chaotically. Motion on vague tori can lead to very long trapping times and highly correlated motion.

In the foregoing, it has been shown how the behavior of the reactive flux can be correlated with the dynamical structure in phase space. All of the systems studied have the same total energy $E = 1.02\epsilon_0$.

In Figure 9, it is shown how the CSS for a given system ($z = 1$, $\lambda = 2.5$) varied with total energy E. It should be noted that systems A–D in Figure 9 are almost entirely stochastic. In Figure 9, we show how the reactive flux decays for each of these systems. As one goes down the column from system A to system D, the width of the transition zone increases dramatically. The corresponding reactive fluxes show a significant change in behavior, clearly due to the effect of increased width. For system A the flux decays exponentially at long times. For systems B and C the flux acquires much more dynamical structure and oscillatory behavior, and for system D no discernable long time decay exists; there is no separate time scale, and

(13) L. F. Shampine and M. A. Gordon, "Computer Solution of Ordinary Differential Equations", W. H. Freeman, San Francisco, 1975.

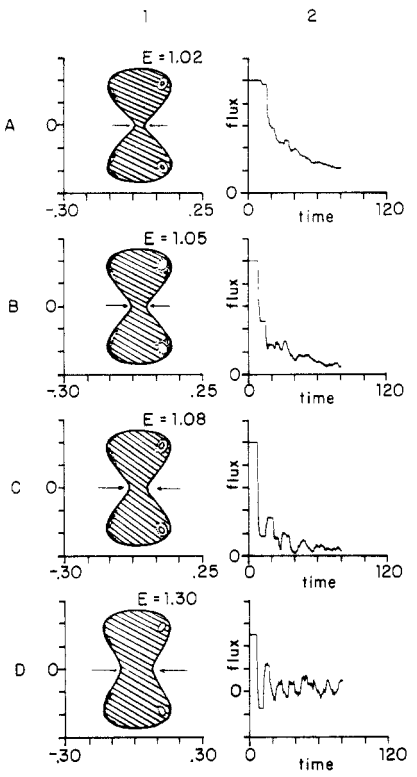

Figure 9. A sequence of configurational surfaces of section and the corresponding reactive fluxes are shown as a function of total energy E. The series corresponds to the system discussed in Figure 7. Arrows indicate the width of the transition zone. The reactive flux changes dramatically as the transition-state zone widens (cf. eq 13) with increasing energy. Note that the measure of irregularity is approximately constant throughout the energy range of interest. In column 1 one tic mark along the y axis corresponds to 0.4 dimensionless units. One tic mark along the flux axis is 0.2 units in A2, B2, and C2 and 0.4 units in D2.

a linear rate law does not apply, even though the extent of stochasticity is more or less constant. Clearly then even for a fully stochastic system when the energy is "too high", a rate constant will not exist. A detailed analysis of this energy dependence shows that, as the total energy is increased, the trapping time decreases because the width of the transition zone increases and the bottleneck effect becomes less pronounced.

Since the canonical reactive flux is

$$k(t;T) = \frac{\int dE\ \Omega(E)k(t,E)e^{-\beta E}}{\int dE\ \Omega(E)e^{-\beta E}}$$

it follows that the dominant contribution to the rate constant stems from energies close to the barrier height. This means that one will see a linear rate law, exponentially decaying flux only for low temperatures.

5. Isomerization in an Isolated *n*-Butane Molecule[14]

To what extent does the information obtained from a detailed study of the two-dimensional model apply to real molecules? Let us consider for a moment the simple isomerization reaction of *n*-butane[8,14]

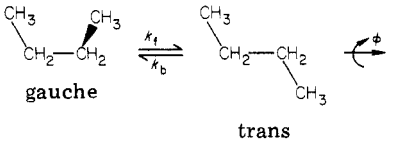

(14) R. O. Rosenberg and B. J. Berne, manuscript in preparation.

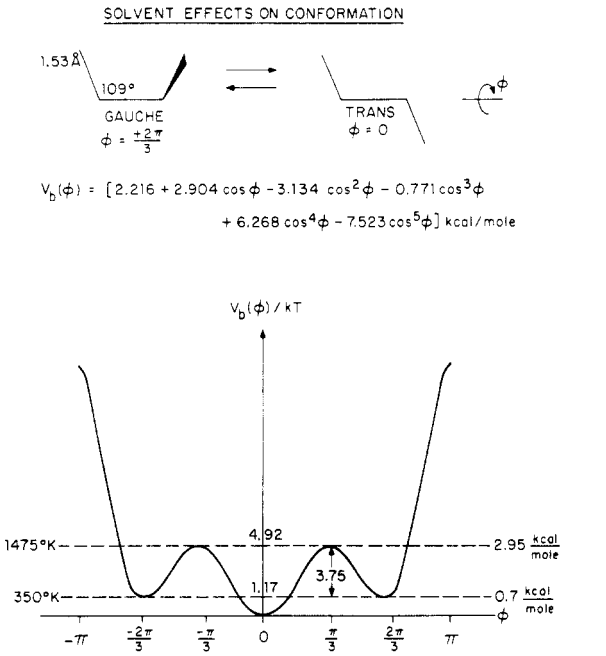

Figure 10. The potential model used to study isomerization dynamics in isolated butane molecules.

in which *n*-butane undergoes a gauche ($\phi = \pm 2\pi/3$) to trans ($\phi = 0$) isomerization reaction. To simplify the study, we ignore the high-frequency C–H stretches, and regard *n*-butane as consisting of four rigid methylene groups. If we label the *n*-butane molecule sequentially, the reaction coordinate is the dihedral angle, ϕ, between the plane containing carbons 1, 2, and 3 and the plane containing carbons 2, 3, and 4. The potential energy for the isolated molecule is[15]

$$V = V_B(\phi) + \tfrac{1}{2}K_b\sum_{i=1}^{3}(b_{i+1,i} - b_0)^2 + \tfrac{1}{2}K_\theta\sum_{i=1}^{2}(\cos\theta_i - \cos\theta_0)^2 \quad (5.1)$$

The first term corresponds to the potential of the reactive degree of freedom. This is taken to be the potential fitted to experiments by Scott and Scheraga[16] and more recently by Ryckaert and Bellemans[17] and shown in Figure 10. The second and third terms in eq 5.1 specify a harmonic model for the stretching of the C–C bonds (with bond lengths labeled sequentially by b_{21}, b_{32}, b_{43}) and the bending of the C–C–C bond angles (labeled θ_1, θ_2). The harmonic force constants are taken to be $K_b = 3.5 \times 10^7$ J/nm^2 mol, and $K_\theta = 1.8 \times 10^5$ J/mol and the equilibrium bond lengths and bond angles are $b_0 = 1.53$ Å and $\theta_0 = 109°28'$, respectively.

In this potential model, there is no coupling between the internal coordinates of the molecule. The coupling between these modes occurs in the kinetic energy. Of the 12 degrees of freedom in the system, the three degrees of freedom corresponding to the center of mass are not interesting. The kinetic energy couples the remaining nine degrees of freedom giving rise to energy exchange between the reactive degree of freedom and the remaining eight other "bath" degrees of freedom.

In Figure 11A is shown the canonical (constant temperature) reactive flux for the isolated butane molecule.

(15) E. Helfand, Z. R. Wasserman, and T. A. Weber, *J. Chem. Phys.*, **70**, 2016 (1979).
(16) R. A. Scott and H. A. Scheraga, *J. Chem. Phys.*, **44**, 3054 (1966).
(17) J. P. Ryckaert and A. Bellemans, *Chem. Phys. Lett.*, **30**, 23 (1975).

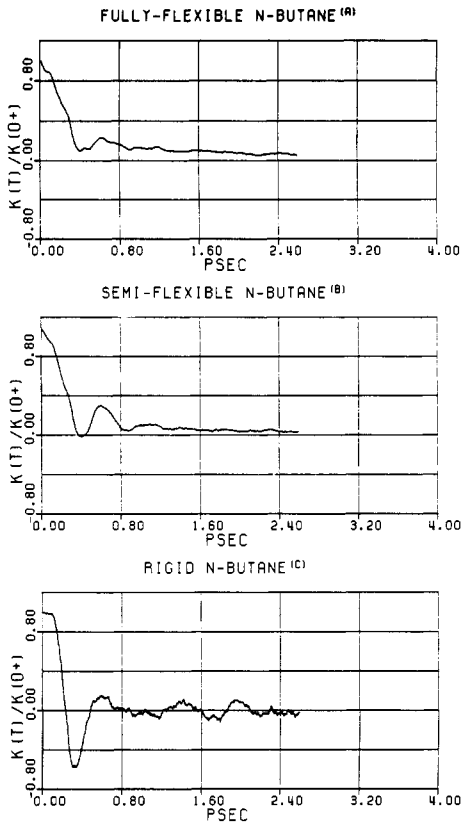

Figure 11. The canonical reactive flux at temperature 300 K for isolated *n*-butane. (a) In the fully flexible moleule, all degrees of freedom are active. (b) In the semiflexible molecules, the C–C bonds are frozen at their equilibrium bond lengths, but all other degrees of freedom are active. (c) In the rigid molecule, the C–C bond lengths are frozen at their equilibrium angles, and the two C–C–C bond angles are frozen at their equilibrium angles. All other degrees of freedom are active.

It is clear from this figure that there is a separation of time scales and a corresponding "exponential" decay at long times. The rate constant exists and moreover

$$1/\tau_{\mathrm{Rxn}} \simeq (0.11)1/\tau_{\mathrm{TST}} \tag{5.2}$$

where τ_{TST}^{-1} is the transition-state value.

In the model of *n*-butane, the C–C stretch frequencies are higher than the C–C–C bending frequencies. To what extent do these higher frequency modes contribute to the energy exchange and thereby to the reaction rate? In Figure 11B is shown the reactive flux for an isolated butane molecule in which the C–C bond lengths are rigid, that is, the higher frequency modes are frozen out. It is clear from a comparison of parts A and B of Figure 11 that, when the C–C stretch is frozen out, the reactive decay still displays a long time "exponential decay" and rate constants still exist; however, the rate constant is a much smaller fraction of the transition-state rate constant. It is important to recognize that the TST rate constants are different for the fully flexible molecule and for the semiflexible molecule. Figure 11C shows the reactive flux for the case when both the bond-bending and bond-stretching modes are frozen out. This is the case of a "rigid" *n*-butane. The kinetic energy couples the reactive coordinate to the molecular rotations. Now we see no long time exponential tail. Hence rate constants do not exist. Thus molecular rotations do not provide an adequate bath.

It is clear from the foregoing that energy transfer is sufficient in realistic isolated molecules to give rise to unimolecular rate laws and rate constants—but rate constants that are not given by RRKM or transition state theory.

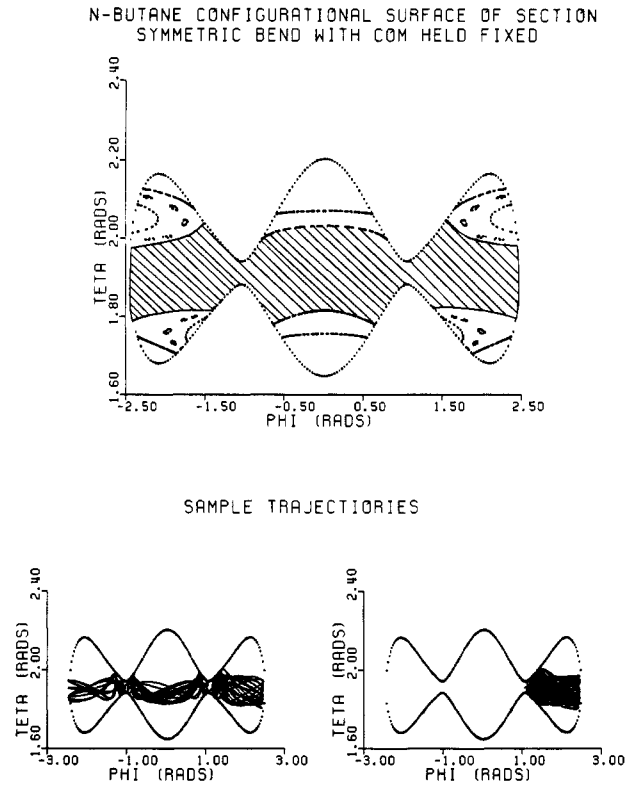

Figure 12. The configurations surface of section of a model of butane in which only the symmetric bending mode and the dihedral angle are allowed to vary. The thatched area indicates that both CT and some TT are destroyed. Two typical reactive trajectories are indicated below. Note that these trajectories can get trapped.

Since the molecular rotations do not provide an adequate bath, we have removed these rotations and have studied the three-dimensional system (ϕ, θ_1, θ_2). This system displays the irreversible decay evinced by the full system, and rate constants still apply. By choosing either the symmetric bend and ϕ or the asymmetric bend and ϕ we have been able to study "realistic" two-dimensional systems. There are many surprises. These are outlined in a manuscript presently in preparation. Suffice it to say that the analysis is based on the concept of TT, CT, and vague tori. To give some feeling for this, the two configurational surfaces of section are presented in Figures 12 and 13. In Figure 12, the CSS corresponding to the two-dimensional system consisting of the symmetric bend and the dihedral angle shows that all the crossing tori and a large measure of trapping tori are destroyed. Typical reactive trajectories are shown. The motion is sufficiently irregular to give rise to rate constants. In Figure 13, the CSS corresponding to the two-dimensional system (at the same energy as the preceding calculation) consisting of the asymmetric bend and the dihedral angle shows that the system is integrable; no tori are destroyed. The trajectories are quasiperiodic. Rate constants do not exist. Clearly care must be taken in reducing a many degree of freedom system to a few degree of freedom system.

6. Discussion

Even in systems consisting of only two degrees of freedom, it has been shown here that nonlinear coupling can give rise to a unimolecular rate law for isomerization and correspondingly to well-defined rate constants. It has also been shown that calculation of the long time decay of the reactive flux allows one to determine the rate constants—should they exist. This has been clearly shown for the most stochastic system (E) of Figure 7 and in this case the RRKM rate constant ($\tau_{\mathrm{RRKM}}^{-1}$) is in excellent

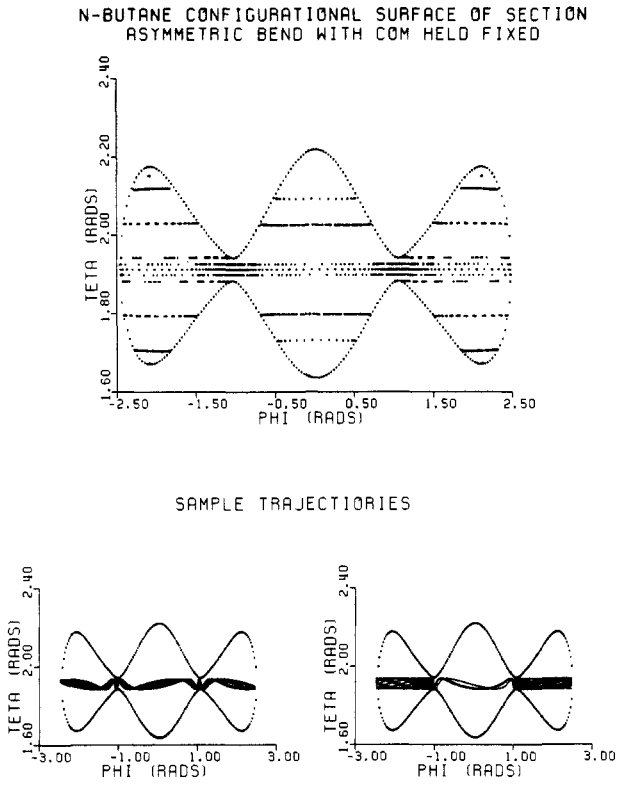

Figure 13. Similar to 12, but now only asymmetric bending mode and dihedral angle is considered. This CSS is at the same energy as in Figure 12. Note that no tori are destroyed.

agreement with the rate constant determined from the reactive flux. The less stochastic system, B–D, of Figure 7, however, exhibits features which cannot be accounted for by simple statistical theory. When the coupling is strong enough to destroy some trapping tori, reactive trajectories do indeed get trapped for long periods of time. These trajectories are irregular but nevertheless display a great deal of coherence; that is, there are very long correlation times. The trapping times appear to be nonrandom and it would take a very long integration time to establish whether these systems are described by a unimolecular rate law with well-defined rate constants. It is possible that the very long time decay in these systems is not exponential—although we suspect it is. There are comparable cases in transport theory—such as Brownian motion in two dimensions—where phenomenological decay is not observed.[18] The reason for the long correlation times and long trapping times in these moderately coupled systems is rather difficult to pin down. What is clear is that a substantial fraction of the crossing trajectories in these systems, although irregular, spend considerable periods of time executing coherent or "regular" motion. The trajectories seem to fall under the influence of the trapping tori that still exist in the system. One consequence of this is that τ_{Rxn} seems to be a decreasing function of the coupling. This behavior is counterintuitive in that we expect the trapping time to increase as the stochasticity (measure of the iregular region of phase space) increases (cf. discussion in section II and Figure 2).

That τ_{Rxn}^{-1} increases as the coupling increases is also consistent with the following argument. In any coupled system energy is exchanged between the x and y oscillators. Let τ_E denote the correlation time of the energy fluctuation—should a correlation time exist. τ_E^{-1} plays a role in this problem somewhat similar to the collision rate, or friction constant, in stochastic dynamic models of barrier crossing. In the event that $\tau_E >> T$, where T is the period of oscillation of a peridic crossing orbit, then a trajectory starting at the transition state will coherently or periodically recross the transition state for a time on the order of τ_E before losing enough energy to get trapped. It will remain trapped until it gains enough energy to recross the barrier. The time of trapping is thus also τ_E and $\tau_{Rxn} \propto \tau_E$ or $\tau_{Rxn}^{-1} \sim \tau_E^{-1}$. Thus we expect the kinetic rate constant τ_{Rxn}^{-1} to be an increasing function of τ_E^{-1}. Intuitively we expect τ_E to decrease and τ_{Rxn}^{-1} to increase as the coupling (stochasticity) increases, an expectation entirely in agreement with the observation. Of course, no evidence is given for the existence of τ_E. These considerations raise more questions than can be answered here, and further study is required.

The simple systems presented here have a rather rich dynamical structure. The focus of this paper has been to clarify the relationship between a reaction dynamics and the dynamical structure associated with the KAM theorem. In fact we know no other work that dicusses this relationship between the topology of phase space and rate constants for barrier crossing in bounded systems. Many of the conclusions outlined here form the basis for further investigations. For example, (a) what happens when there are more than two degrees of freedom; (b) what are the dynamics in a corresponding quantum system? With regard to (a), it is important to elucidate the role of Arnold diffusion. With regard to (b), it has already been shown that there is a transition to chaos in wave packet dynamics. Nevertheless, this remains a controversial area. It also enables one to pose an exact quantum counterpart to the RRKM theory.

In closing we reiterate that, for very strongly coupled systems, that is, systems in which all the tori are destroyed and the energy is close to the barrier, a unimolecular rate law pertains, rate constants exist, and the rate constants are very well approximated by RRKM (transition-state) theory. It is interesting to not that this suggests that we explore the conditions under which all trapping tori are destroyed. By applying linear stability analysis to the "most stable" elliptic point, we have recently been able to predict when RRKM behavior should be expected.[19]

Appendix A. A Statistical Theory of Rate Constants in Nonergodic Systems

Phase space is decomposable into regular and irregular parts. Let us define a quantity $I(\Gamma)$ which has the property that

$$I(\Gamma) = 1 \quad \Gamma \in S_I$$
$$= 0 \quad \Gamma \notin S_I \tag{A1}$$

where S_I is the measurable set of irregular points in phase space. Let us define the normalized microcanonical density on the subspace S_I as

$$\rho_I(\Gamma \cdot E) = \frac{1}{\Omega_I(\Gamma)} \delta(E - H(\Gamma)) I(\Gamma) \tag{A2}$$

where

$$\Omega_I(\mathbf{E}) = \int d\Gamma \, I(\Gamma) \delta(E - H(\Gamma)) \tag{A3}$$

is the density of irregular states at energy E. Let us now define the normalized autocorrelation function of the fluctuation in product molecules

$$C_I(t;E) = \langle \delta N_B(0) \delta N_B(t) \rangle_{E,I} / \langle \delta N_B^2 \rangle_{E,I} \tag{A4}$$

where subscript E,I indicates an average over ρ_I; that is,

(18) J. H. Dymond and B. J. Alder, *J. Chem. Phys.*, 52, 923 (1970).

(19) N. De Leon and B. J. Berne, *J. Chem. Phys.*, in press.

over the irregular part of phase space. The corresponding reactive flux is

$$k_I(t;E) = -\frac{d(C_I(t;E))}{dt} = \frac{\langle \dot{y}(0)\delta(y(0) - y_c)\theta(y(t))\rangle_{E,I}}{\langle \theta(y)\rangle_{E,I}[1 - \langle \theta(y)\rangle_{E,I}]} \quad (A5)$$

This follows from the uniformity of the propagator and the stationarity of $\rho_I(\Gamma,E)$. The latter follows from the fact that I is a constant of the motion (a regular trajectory remains regular, and an irregular trajectory remains irregular, and never the twain shall meet). It is also easy to show that from symmetry $\langle \theta(y)\rangle_{E,I} = x_B = 1 - \langle \theta(y)\rangle_{I,E} = x_A$. Every trajectory contributing to $k_I(t;E)$ is a crossing trajectory. The initial value of this reactive flux is

$$\frac{1}{\tau_{BD}} \equiv \lim_{t\to 0^+} k_I(t;E) = \frac{1}{x_A x_B}\langle \dot{y}\theta(\dot{y})\delta(y - y_c)\rangle_{E,I} \quad (A6a)$$

$$\frac{1}{\tau_{BD}} = \frac{1}{x_A x_B}\frac{\int d\Gamma\, I(\Gamma)\delta(E - H(\Gamma))\dot{y}\theta(\dot{y})\delta(y - y_c)}{\int d\Gamma\, I(\Gamma)\delta(E - H(\Gamma))} \quad (A6b)$$

If all the crossing trajectories are irregular then $I(\Gamma)$ can be deleted from the numerator and

$$\frac{1}{\tau_{BD}} = \frac{1}{x_A x_B}\frac{1}{\Omega_I(E)}\int d\Gamma\, \delta(E - H(\Gamma)\dot{y}\theta(\dot{y})\delta(y - y_c) \quad (A7a)$$

$$\frac{1}{\tau_{BD}} = \frac{\Omega(E)}{\Omega_I(E)}\frac{1}{\tau_{RRKM}} \quad (A7b)$$

A statistical theory of the rate constant is formulated as follows: Each trajectory originating at the transition state, y_c, gets trapped for a time (long compared to vibrational periods) in the well toward which it is initially moving. Then there are no rapid recrossings. A trapped trajectory can only recross after it regains energy from the other degrees of freedom (to which the energy was originally lost). The distribution of trapping times is assumed to be random. Then $C_I(t;E)$ must decay as a single exponential and since its initial decay rate is given by eq A6, it follows that

$$k_I(t;E) = \frac{1}{\tau_{BD}} e^{-t/\tau_{BD}} \quad (A.8)$$

Thus the decay rate of $k_I(t;E)$ is $1/\tau_{BD}$. If the whole energy hypersurface is irregular

$$\frac{1}{\tau_{BD}} \to \frac{1}{\tau_{RRKM}} = \frac{1}{x_A x_B}\frac{1}{\Omega(E)}\int d\Gamma\, \delta(E - H)\dot{y}\delta(y - y_c)\theta(\dot{y}) \quad (A.9)$$

Now in an experiment, suppose the initial states are microcanonically distributed according to $\rho(\Gamma) = \delta(E - H)/\Omega(E)$. Since

$$\rho(\Gamma) = \frac{[I + (1 - I)]\delta(E - H)}{\Omega(E)} = \frac{\Omega_I(E)}{\Omega(E)}\rho_I(\Gamma,E) + \frac{\Omega_R(E)}{\Omega(E)}\rho(E) \quad (A.10)$$

where $\Omega_R(E) = \Omega(E) - \Omega_I(E)$ is the density of regular states and $\rho_R(\Gamma,E) = (1 - I)\delta(E - H)/\Omega_R(E)$.

The full fluctuation correlation function is

$$C(t,E) = \frac{\langle \delta N_B(0)\delta N_B(t)\rangle_E}{\langle \delta N_B{}^2\rangle_E} \quad (A.11)$$

where the average is over the full energy hypersurface. Upon substitution of eq A.10, this can be expressed as

$$C(t) = \frac{\Omega_I(E)}{\Omega(E)}C_I(t;E) + \frac{\Omega_R(E)}{\Omega(E)}C_R(t;E) \quad (A.12)$$

where

$$C_R(t;E) = \frac{1}{x_A x_B}\int d\Gamma\, \delta(E - H(\Gamma))[1 - \underset{\uparrow}{I(\Gamma)}]\delta N_B(0)\delta N_B(t) \quad (A.13)$$

regular trajectories

Now if all crossing trajectories are irregular, none of the trajectories contributing to $C_R(t;E)$ can cross the barrier so that $C_R(t;E)$ is constant in time; that is, $C_R(t;E) = C_R(0,E)$. It follows from eq A.12 that the reactive flux will then be

$$k(t;E) = -\frac{d(C(t))}{dt} = \frac{\Omega_I(E)}{\Omega(E)}k_I(t;E) \quad (A.14)$$

Substitution of eq A.8 into eq A.14 then gives the reactive in the statistical theory

$$k(t;E) = \frac{\Omega_I(E)}{\Omega(E)}\frac{1}{\tau_{BD}} = \frac{1}{\tau_{RRKM}}e^{-t/\tau_{BD}} \quad (A.15)$$

where the last equality follows from eq A.7b.

This shows that the exponential decay observed in a nonergodic system in which all crossing trajectories are irregular is given by decay constant $1/\tau_{BD}$ defined in eq A7b and 2.7. When there are TT, $\Omega_I(E) < \Omega(E)$ so that

$$1/\tau_{BD} > 1/\tau_{RRKM} \quad (A.16)$$

but when the measure of all TT is zero

$$1/\tau_{BD} = 1/\tau_{RRKM} \quad (A.17)$$

It is important to note that the prefactor of the exponential in eq A.15 is $1/\tau_{RRKM}$. Thus, in general, the statistical decay rate cannot be found from the initial time derivative of the full time correlation function.

Acknowledgment. This work was supported by NSF CHE 79-07820, and NIH 9R01 GM 26588-06.